

A Review of Using Transfer Path Analysis Methods to Derive Multi Axis Vibration Environments

Steven Carter

Sandia National Laboratories¹
P.O. Box 5800 – MS0557
Albuquerque, NM, 87185

ABSTRACT

Multi-axis testing has become a popular test method because it provides a more realistic simulation of a field environment when compared to traditional vibration testing. However, field data may not be available to derive the multi-axis environment. This means that methods are needed to generate “virtual field data” that can be used in place of measured field data. Transfer path analysis (TPA) has been suggested as a method to do this, since it can be used to estimate the excitation forces on a legacy system and then apply these forces to a new system to generate virtual field data. This paper will provide a review of using TPA methods to do this. It will include a brief background on TPA, discuss the benefits of using TPA to compute virtual field data, and delve into areas for future work that could make TPA more useful in this application.

Keywords: TPA, force reconstruction, MIMO, vibration testing, environments

INTRODUCTION AND MOTIVATION

Sandia National Laboratories has been investigating and using multi-axis random vibration testing for many years, developing methods and software to perform the tests [1, 2]. However, the processes for developing test specifications that are compatible with multi-axis testing are lacking. Test specifications from traditional random vibration testing cannot be used because they are generally “straight-line” enveloped spectra. These typically include smeared and amplified frequency content that encompasses all the part-part and test-test variation that may be seen in a family of source environments or parts. Additionally, the test specifications may be derived from field test hardware (such as flight test units) that have significantly different structural dynamics than the device under test (DUT). An example of this type of specification is shown in Figure 1, where a straight-line spectrum is used to capture the cargo vibration exposure from a jet aircraft [3].

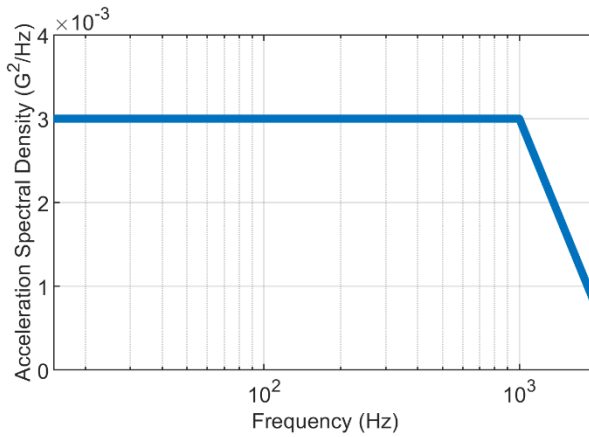


Figure 1: Example enveloped spectra for jet aircraft cargo vibration exposure from MIL-STD 810H

¹Sandia National Laboratories is a multimission laboratory managed and operated by National Technology and Engineering Solutions of Sandia, LLC., a wholly owned subsidiary of Honeywell International, Inc., for the U.S. Department of Energy’s National Nuclear Security Administration under contract DE-NA0003525

This paper describes technical results and analysis. Any subjective views or opinions that might be expressed in the paper do not necessarily represent the views of the U.S. Department of Energy or the United States Government.

While these types of specifications make it easy to build in conservatism and combine data from multiple tests, they are not realizable in a multi-axis sense. This is because the multi-axis controller uses several input degrees of freedom (DOFs) to control several output DOFs. This approach contrasts with the single input/single output (SISO) strategy in traditional vibration testing, which presents a relatively straight forward control problem. An example of a “small” multi-axis test set-up is shown in Figure 2. Larger set-ups that use upwards of twelve shakers (inputs) and thirty output DOFs have become standard at Sandia.

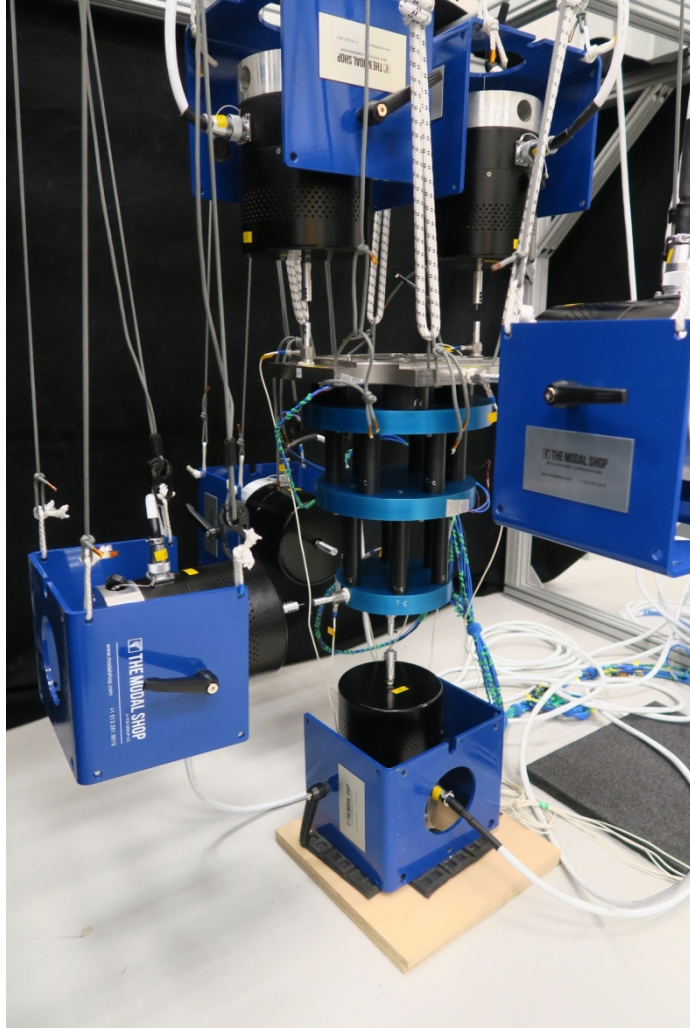


Figure 2: Example multi-axis vibration test set-up

The key difference between SISO and multi-axis control is that a multi-axis test attempts to control the frequency, phase, and amplitude relationships of all the output DOFs, while SISO tests only control the frequency and amplitude at a single DOF. As such, the frequency, phase, and amplitude relationships between the output DOFs (the system structural dynamics) should be the same to for the multi-axis test specification and DUT to perform an accurate test. The reasons for this constraint can be easily understood once the multi-axis control strategy is known.

Equation 1 shows the basic control strategy, where $X(\omega)$ is the square cross power spectral density (CPSD) matrix of target responses (the test specification), $H(\omega)$ is the frequency response function (FRF) matrix that describes input/output relationship between the shaker drive voltages and system responses, and $V(\omega)$ is the CPSD matrix of the shaker drive voltages. Note that the “+” indicates a pseudo inverse and “*” indicates a conjugate transpose.

$$[V(\omega)] = [H(\omega)]^+ [X(\omega)] [H(\omega)]^{+*} \quad (1)$$

This equation makes it clear that there must be compatibility in the structural dynamics between $X(\omega)$ and $H(\omega)$ to find a reasonable solution for $V(\omega)$. This has typically been accomplished by computing the target CPSD matrix from field test data and applying that to the DUT. This approach does not present a complete solution though, since compatibility issues may still be encountered if the field test hardware is significantly different from the DUT or if field test data isn't available (e.g., when deriving environments from legacy hardware). An intuitive understanding of this problem can be gained by picturing a test specification that attempts to force operating deflection shapes to occur at frequencies that are unnatural for the DUT.

Additionally, it is obvious that the DUT must share the same nominal sensor and component configuration as the field data. Otherwise, there is currently no satisfactory technique to map field test responses to the DUT responses. Some methods have been developed to tailor test specifications to fix these compatibility issues [4, 5], and further research is underway. In the absence of a solution to fix these issues, it is easy to picture situations where the test specification is inappropriate for the DUT, resulting in a test that is difficult to control and/or does not represent the true field environment.

This introductory information suggests that it would be a clear advantage to have field data for the exact DUT when deriving multi-axis test specifications. However, the cost and time to perform a field test makes it infeasible in many cases. As such, methods need to be developed to generate "virtual field data" through simulations. This paper presents transfer path analysis (TPA) as a potential simulation method for this. It will provide a brief background on TPA, discuss the benefits and drawbacks, and discuss areas for future work. Note that this paper represents an initial effort into using TPA this way and several improvements are still needed to mature and build trust in the method. Nevertheless, it is felt that this paper provides a unique perspective on the use of TPA and hopes to inspire further research.

TRANSFER PATH ANALYSIS THEORETICAL BACKGROUND

This section will provide a brief background on TPA, but it is suggested that the reader refer to [6] for a more complete description of the method. The first step towards understanding TPA is to grasp the source-path-receiver model of mechanical systems. Figure 3 shows a sketch of a rocket system with clear boundaries for the source, path, and receiver. In this case the propulsion system is the source, the payload is the receiver, and the attachment points between the propulsion system and payload are the paths.

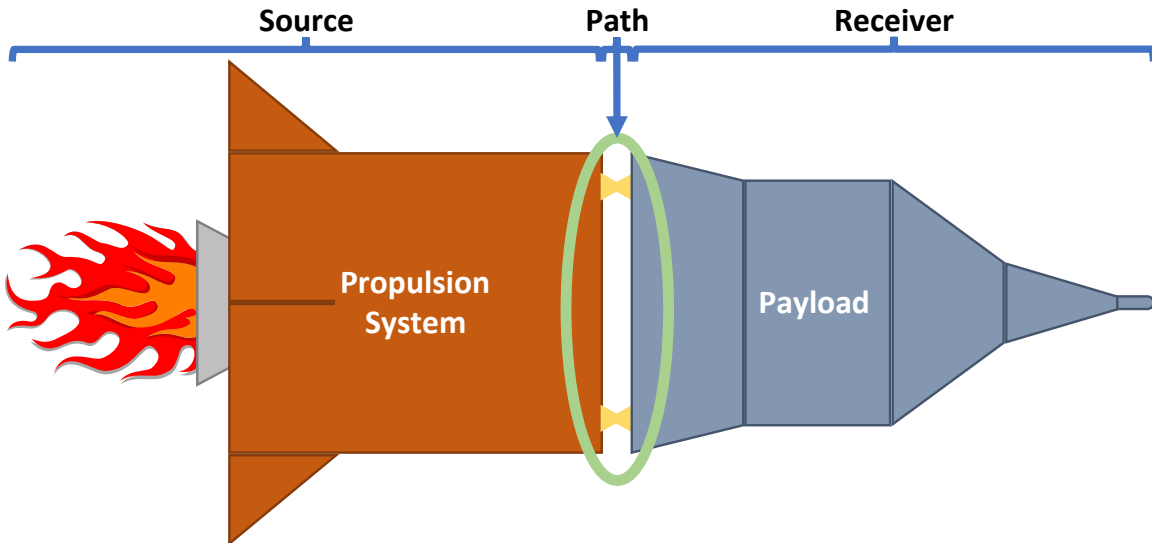


Figure 3: Rocket system sketch showing the source-path-receiver descriptions

The source-path-receiver system can also be described mathematically, as shown in Equation 2 for linear units or Equation 3 for power units. In this case, $X(\omega)$ is the payload response or receiver, $H(\omega)$ are the system FRFs (typically between the

source/receiver attachment points and the measurement locations on the receiver) or paths, and $F(\omega)$ are the forces acting upon the receiver or source.

$$\{X(\omega)\} = [H(\omega)]\{F(\omega)\} \quad (2)$$

$$[X(\omega)] = [H(\omega)][F(\omega)][H(\omega)]^* \quad (3)$$

The forces acting upon the receiver system can then be estimated via FRF matrix inversion, as shown in Equation 4 for linear units or Equation 5 for power units. Like Equation 1, the “+” indicates a pseudo inverse and “*” indicates a conjugate transpose. Note that this paper will only focus on the matrix inversion method for determining the forces.

$$\{F(\omega)\} = [H(\omega)]^+\{X(\omega)\} \quad (4)$$

$$[F(\omega)] = [H(\omega)]^+[X(\omega)][H(\omega)]^* \quad (5)$$

The TPA methods can be broken down into two fundamental techniques once the source-path-receiver concept is understood. These techniques are typically referred to as classical or component-based TPA [6]. Both techniques use the same fundamental math and response measurements to estimate the forces, but with different FRFs representing the paths. Classical TPA uses a representation of the system that relies on the receiver system only (i.e., the FRFs are derived from the receiver system decoupled from the source system); a sketch of this representation is shown in Figure 4.

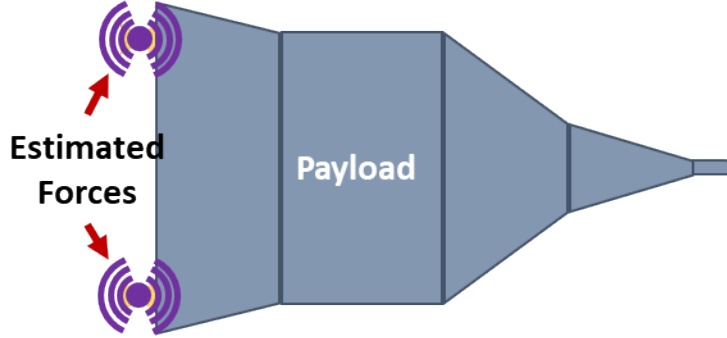


Figure 4: Rocket system representation for classical TPA

The estimated forces from classical TPA are representative of the actual loads experienced in the joint during the field test. In essence, the forces are analogous to load cells between the source and receiver system during the field test. While interesting from a diagnostic perspective, these forces are dependent on the structural dynamics of both the source and receiver systems. As such, they will change as the structural dynamics change in the receiver system. This means that the response prediction on a new receiver may be inaccurate, depending on the differences in the structural dynamics between the new and original systems.

Component-based TPA uses the coupled source-receiver representation of the system (i.e., the FRFs are derived from the coupled source-receiver system), a sketch of this representation is shown in Figure 5. In this case, the estimated forces represent “equivalent sources” that cancel out the effects of the true source on the receiver system. It can be shown that these forces are a property of the true source and the FRFs between the true source and equivalent source [6]. As such, these forces can be applied to any version of the coupled source-receiver system if the source system remains the same. It is important to note that the bounding boxes that define the source and receiver systems can be somewhat arbitrary. However, practicality will generally dictate the boundary, based on what makes sense or is easy to keep the same between versions of the coupled source receiver system.

The underlying theory means that the predicted response from the equivalent sources is theoretically the same as the true field environment. It is also important to note that the equivalent sources can be estimated anywhere on the source system and are not limited to the source/receiver interface points. Additionally, it should be noted that the equivalent sources cannot be used

to predict responses on the source system. Again, the reader is referred to [6] for a derivation of the equivalent source concept that has a more detailed discussion of the assumptions and requirements. Lastly, the reader should be aware that the equivalent sources are referred to by many names, such as blocked forces, interface forces, or pseudo forces, depending on where the forces are on the source system, how they were estimated, author preferences, etc.

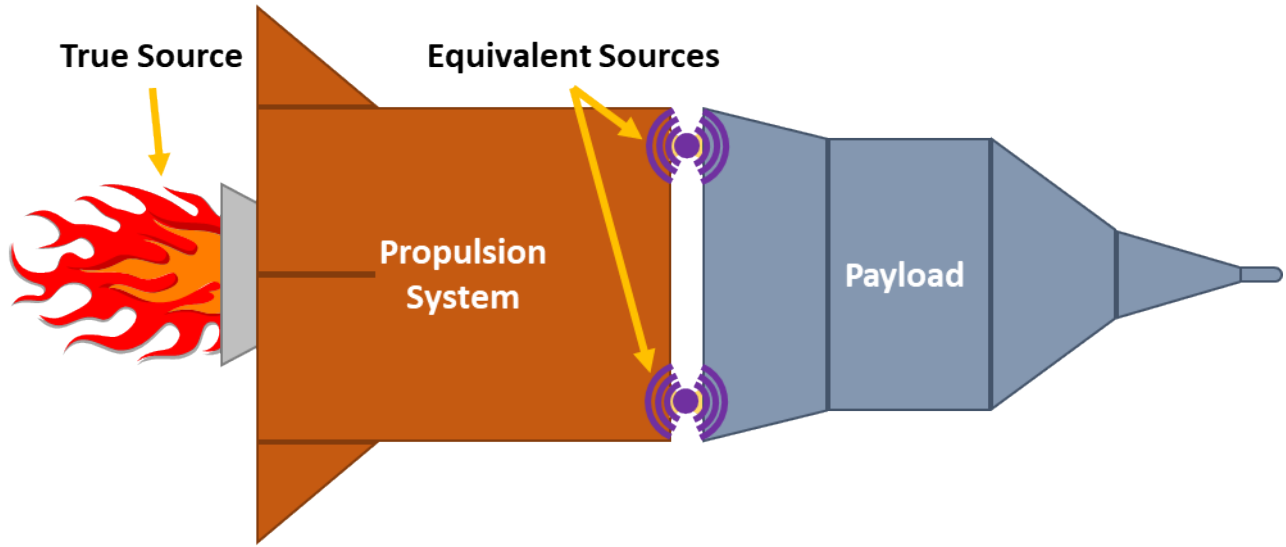


Figure 5: Rocket system representation for component-based TPA

Both versions of TPA present value for deriving virtual field data, but component-based TPA clearly provides the most value since it results in a true estimate of the field environment. This assertion will be discussed more in the following sections.

EXAMPLE ON A BASIC SYSTEM

The TPA process to generate virtual field data will be demonstrated on finite element (FE) models of the round robin system from the Society for Experimental Mechanics (SEM) Dynamic Substructures Technical Division, as described in [7, 8]. This system is shown in Figure 6 and is composed of a frame and wing. There are “thick” wing and “thin” wing versions of the system, which provides an original (thick wing) system to estimate the forces on and a new (thin wing) system for predicting virtual field data.

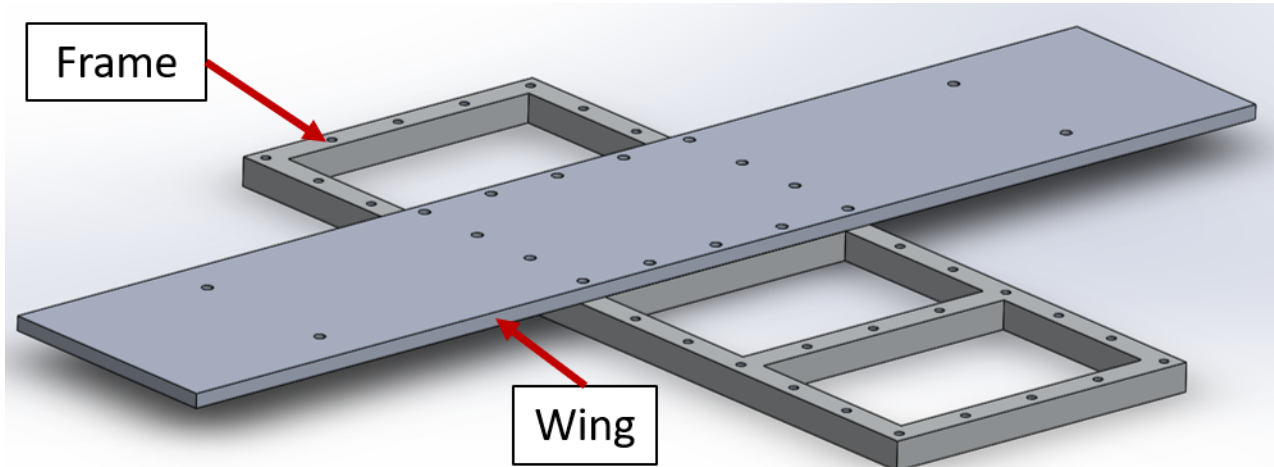


Figure 6: Computer aided design model of the round robin system

The FE model was generated with Sandia's in-house finite element analysis software, Sierra/SD, and the FRFs were generated from the computed modes with a damping ratio of 0.5%. Bolted joints between the frame and wing were simulated with JOINT2G elements that were rigidly connected to the bolt holes on the frame and wing at the interface points that are highlighted in Figure 7. Note that the JOINT2G elements are analogous to a Nastran CBUSH element. Additionally, the JOINT2G spring properties were chosen to represent a typical bolted connection. More information on the models can be found in [9].

The workflow for evaluating the different TPA techniques was as follows:

1. Triaxial broadband excitation was applied to the corners of the frame, as shown in Figure 8, to generate truth data for both versions of the system. This was done using model derived FRFs (from the mode shapes) at 24 triaxial response locations (72 response DOFs) that were evenly distributed over the wing using engineering judgement. Note that the number of response DOFs was chosen to have a reasonable overdetermination ratio between the response and reference DOFs.
2. The (triaxial) forces were then estimated for the thick wing (original) system at the interface locations, as shown in Figure 7. The FRFs were derived from the coupled frame/wing system for the component-based TPA technique (with the frame side interface node as the reference). The FRFs were derived from the wing-only model (at the wing side interface node) for the classical TPA technique.
3. The “virtual field data” was then generated for the thin wing (new) system using the FRFs derived from the appropriate models (frame/wing or wing alone) for the different force estimates.

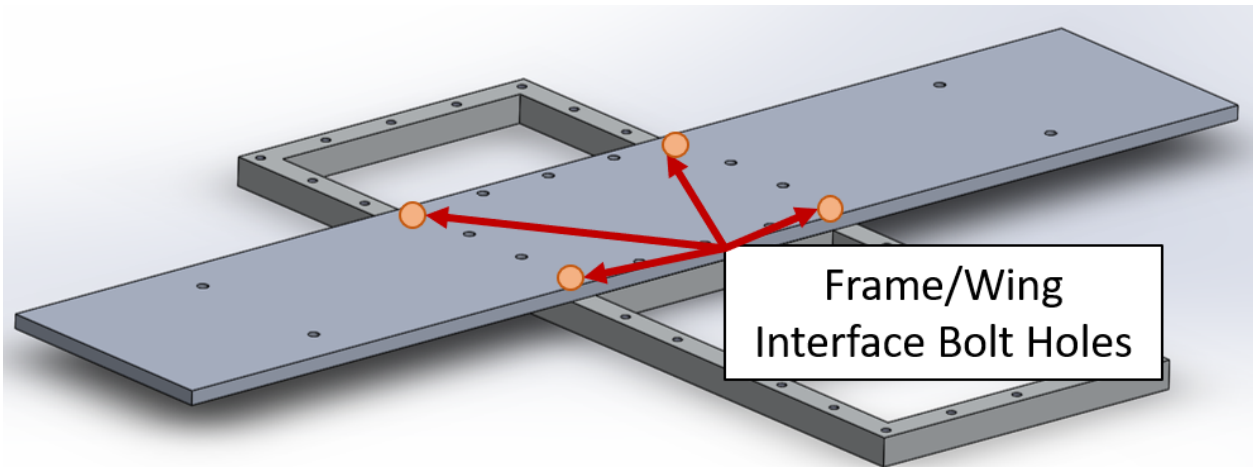


Figure 7: Frame/wing interface points on the round robin system

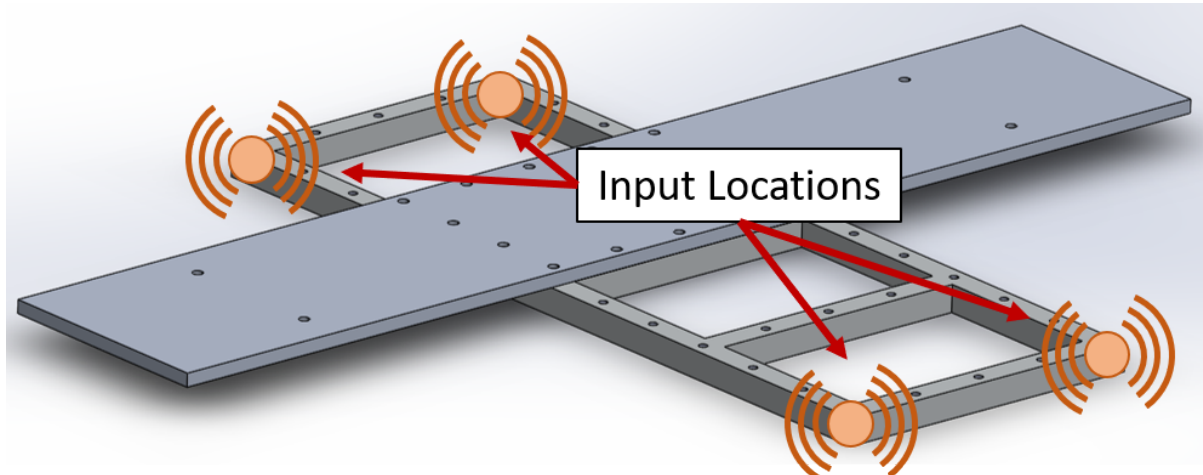


Figure 8: Input locations for the virtual flight test

Figures 9-12 show the auto-power spectral densities (APSDs) that were found from the process described above. Figure 9 and Figure 10 show the results for the component-based and classical TPA on the thick wing (original) system (this response reconstruction is typically done as a check on the force estimation process). Figure 11 and Figure 12 show the results for the component-based and classical TPA on the thin wing (new) system. All the plots show the maximum enveloped spectrum, minimum enveloped spectrum, and averaged spectrum for all the response DOFs to summarize all the APSDs.

All the results are as expected. Both classical and component-based TPA appear to be accurate on the thick wing (original) system (the one that was used to estimate the forces), based on the accuracy of the virtual field data compared to the truth data. This agreement provides a minor validation of the force estimates and is primarily a check on the least square solution for the forces (i.e., checking that the math worked as intended, *not* checking the validity of the forces). The response prediction from component-based TPA is extremely accurate for the thin wing (new) system (which the environment is being “translated” to). However, there are significant errors in the classical TPA response predictions, as expected. In general, the classical TPA response prediction appears to overestimate the thin wing response. This overprediction is likely due to the thin wing being lighter and more flexible than the thick wing and isn’t representative of a general trend in classical TPA.

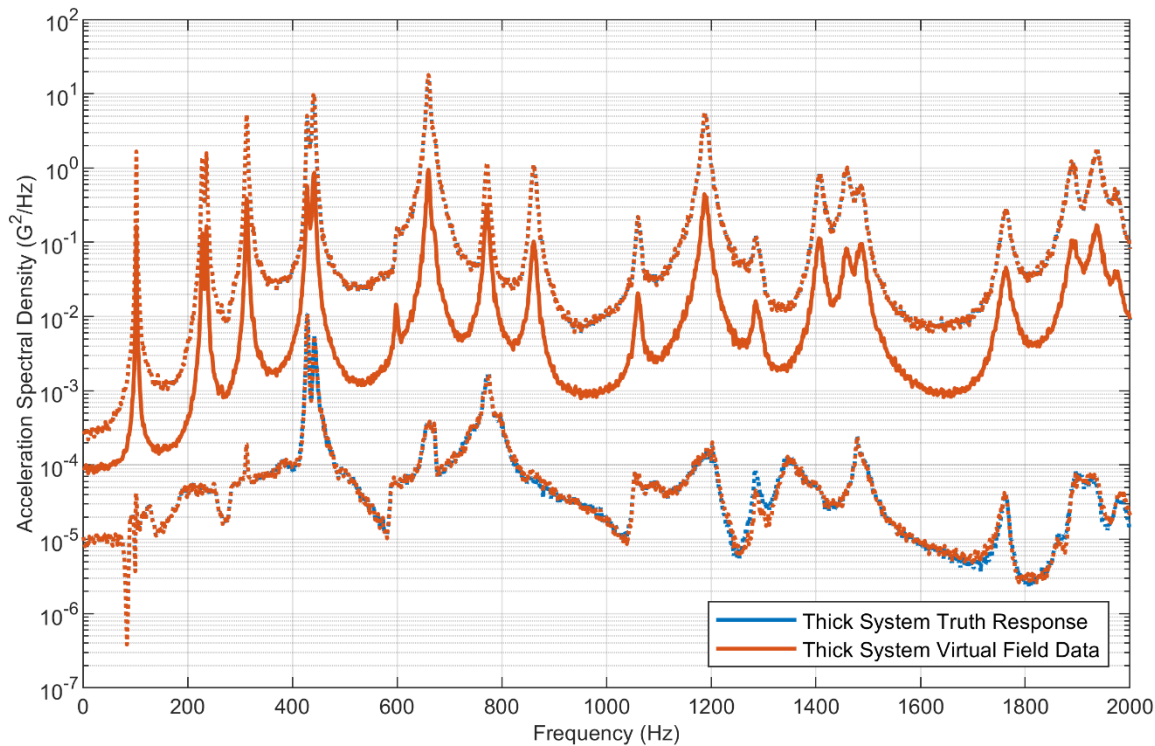


Figure 9: Comparison between the truth and virtual field data for the thick wing (original) system using component-based TPA, the dashed lines represent the maximum and minimum enveloped APSD response, and the solid line represents the averaged APSD response

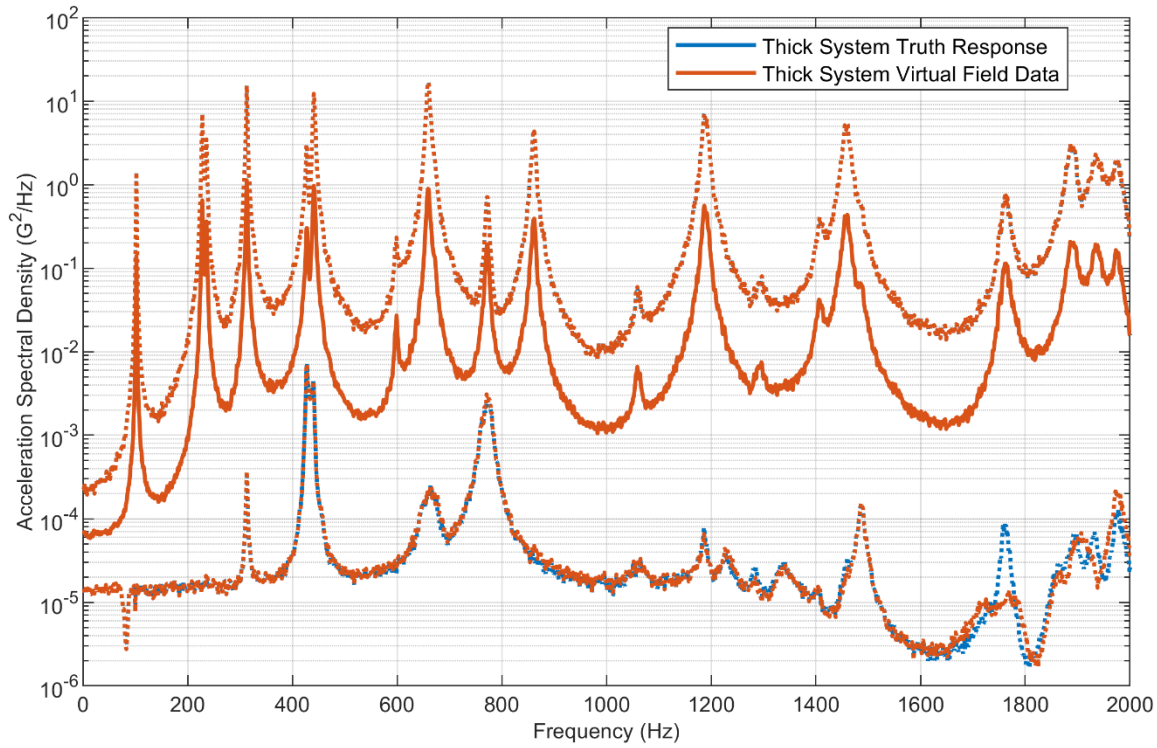


Figure 10: Comparison between the truth and virtual field data for the thick wing (original) system using classical TPA, the dashed lines represent the maximum and minimum enveloped APSD response, and the solid line represents the averaged APSD response

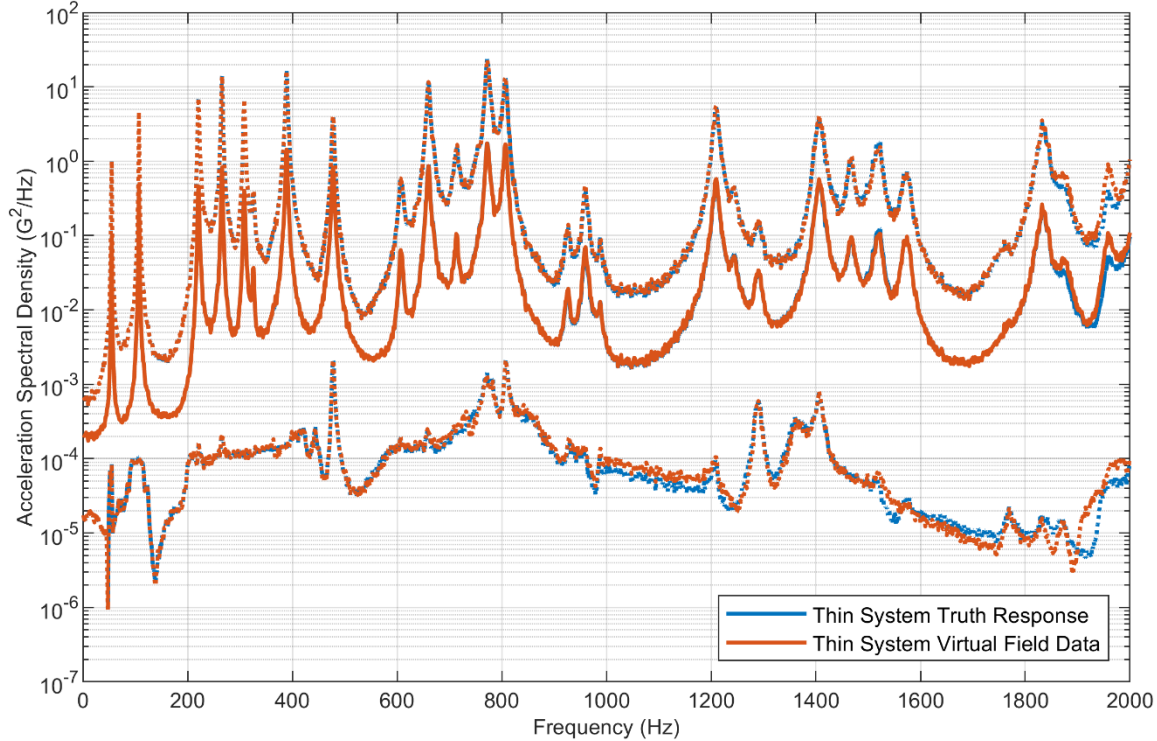


Figure 11: Comparison between the truth and virtual field data for the thin wing (new) system using component-based TPA, the dashed lines represent the maximum and minimum enveloped APSD response, and the solid line represents the averaged APSD response

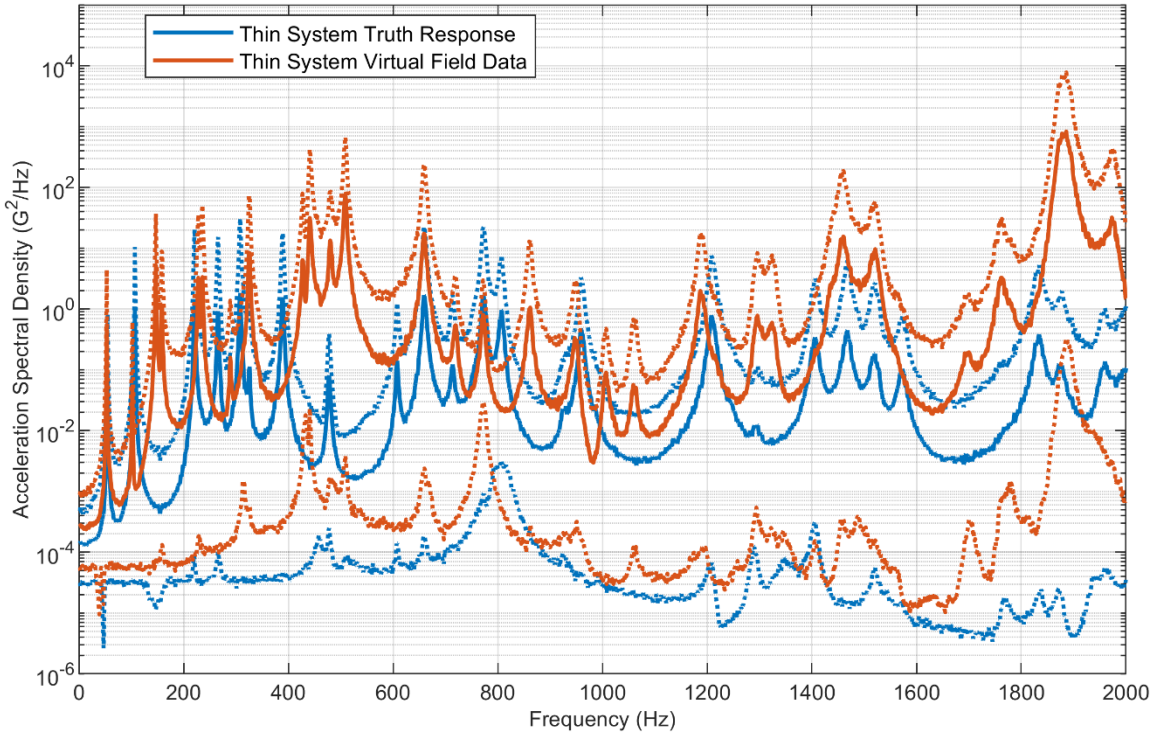


Figure 12: Comparison between the truth and virtual field data for the thin wing (new) system using classical TPA, the dashed line represents the maximum and minimum enveloped APSD response, and the solid lines represent the averaged APSD response

DISCUSSION

As expected, the above results clearly show that component-based TPA is the preferred solution for translating vibration environments from one system to another. This preference is because it provides a highly accurate prediction of the vibration response on the new system, assuming that the appropriate data is available to derive the necessary FRFs. Unfortunately, models of the source system (either FRFs, mode shapes, or FE models) may not be available, making component-based TPA impossible. Classical TPA provides an alternative in this case since it only requires a model of the receiver system.

However, there is a clear trade-off in accuracy, since classical TPA shows significant errors when compared to the truth data. While this inaccuracy causes obvious problems for specification derivation, it is important to keep in mind that the alternative may be the direct application of the thick wing (original) system data to the thin wing (new) system. In this case, the classical TPA response predictions may provide a better specification, since it will generally be more realizable than the original system response. This advantage is because the classical TPA response prediction will “build in” the structural dynamics of the new system rather than trying to enforce the structural dynamics of the original system on the new system (as described above).

This outcome is clearly seen in the results of a synthesized thin wing multi-axis test, as shown in the figures below (note that this is a “test” of the thin wing by itself). Figure 13 shows the “test” APSD results when the thick wing (original coupled frame/wing) system CPSD is used as a test specification. Figure 14 shows the test PSD results when the thin wing (new wing) classical TPA based CPSD is being used as a test specification. Figure 15 shows the test APSD results when the thin wing (new coupled frame/wing) system truth CPSD is used as a test specification (to show that control is possible when the true response is used). Note that the multi-axis control strategy is finding forces rather than voltages in this case, but that it is still using Equation 1 to estimate the sources.

Additionally, both TPA techniques can predict responses at locations that may exist in the new system but didn’t exist in the original system. This capability can also be used to provide a richer set of response targets for the specification, which may improve the accuracy of the inverse source estimation in the multi-axis control strategy.

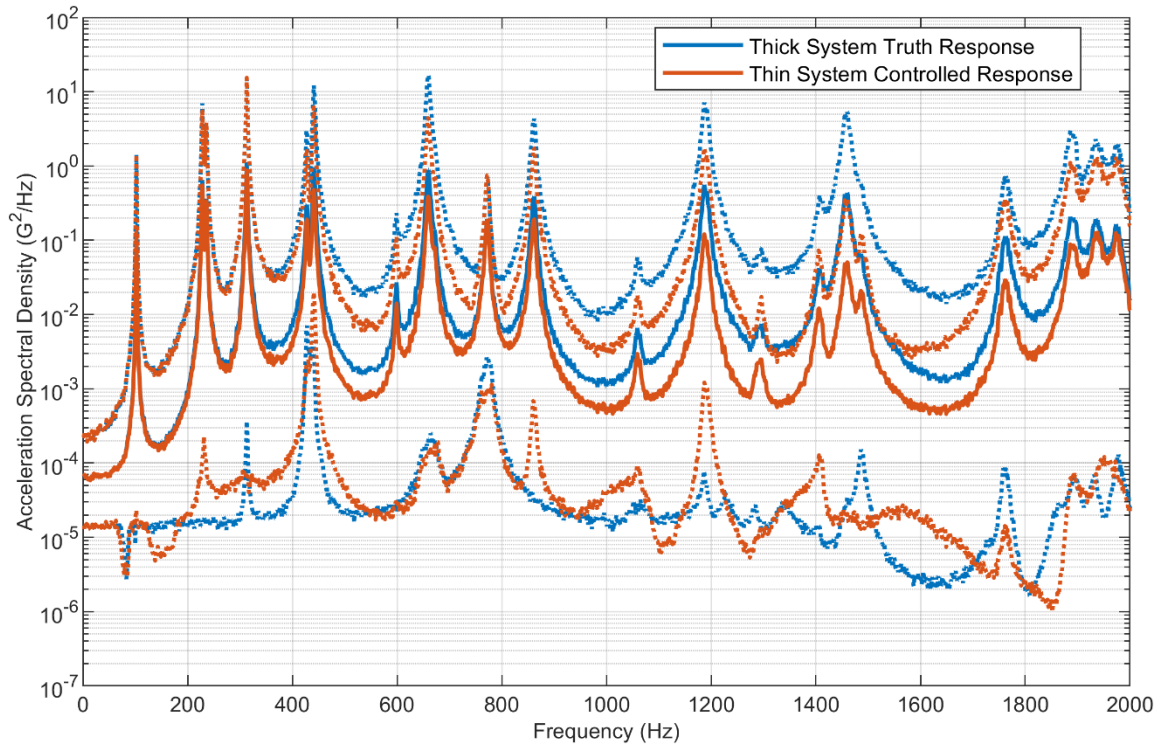


Figure 13: Example of an attempt to control a multi-axis test on the thin system using the thick system CPSD as a test specification, the dashed line represents the maximum and minimum enveloped APSD response, and the solid line represents the averaged APSD response

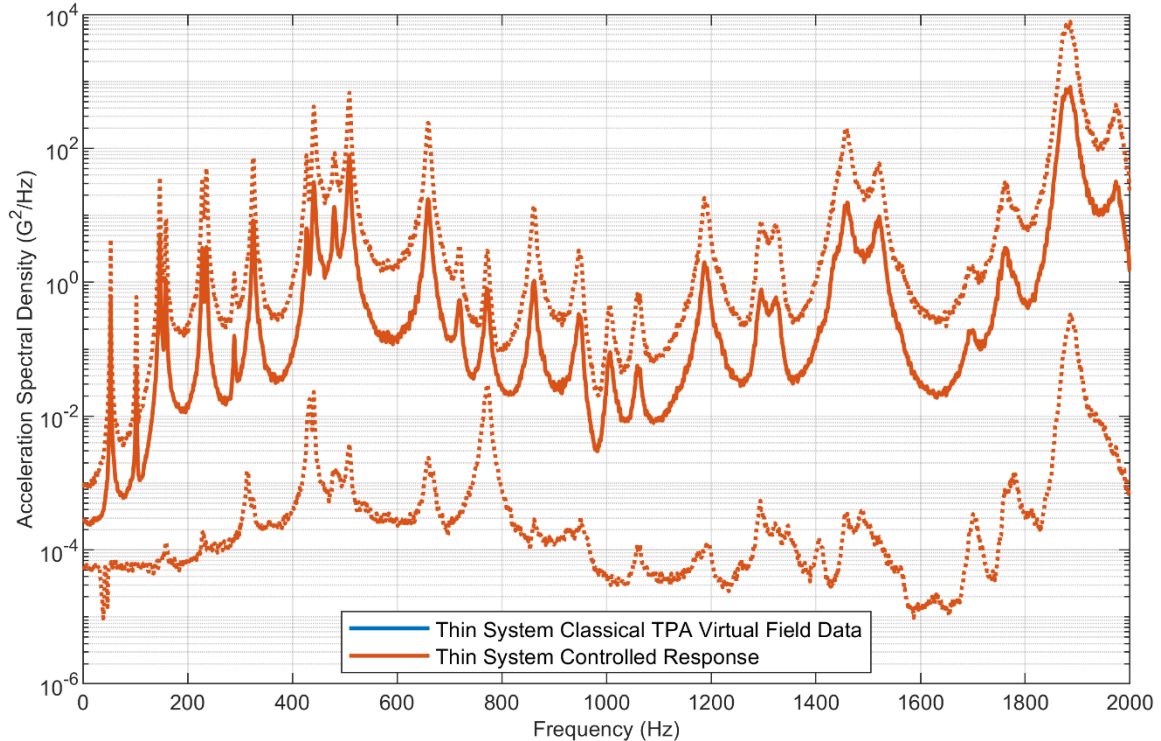


Figure 14: Example of an attempt to control a multi-axis test on the thin system using the classical TPA based response (CPSD) estimation as a test specification, the dashed line represents the maximum and minimum enveloped APSD response, and the solid line represents the averaged APSD response

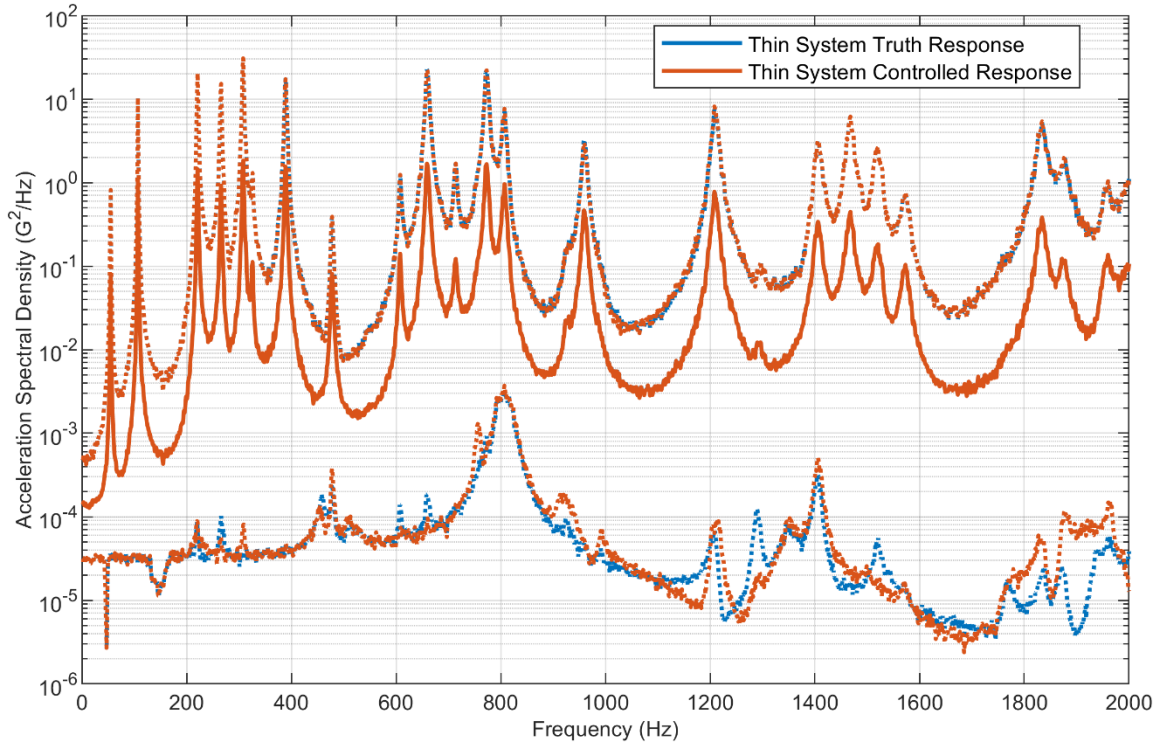


Figure 15: Example of an attempt to control a multi-axis test on the thin system using the thin system truth CPSD as a test specification, the dashed line represents the maximum and minimum enveloped APSD response, and the solid line represents the averaged response

AREAS FOR FUTURE WORK

TPA shows significant promise for generating virtual field data for developing multi-axis test specifications, but there are several areas for future work to build trust in the method. One major area of future work should be developing methods for choosing appropriate FRFs for the inverse force estimation. Satisfactory methods have been developed for the determination of the response DOFs [10], but choosing appropriate reference (or pseudo-force) DOFs seems to be an open area of research.

The importance of choosing appropriate references has been highlighted in recent work [9]. It was shown that having inappropriate references in the FRF matrix could lead to an overfit solution. This causes significant errors in the response predictions when translating the environments to a new system (with component-based TPA). Some methods have been suggested to guide the choice of FRFs and validate the estimates [11], although these methods focused on improving the numerical conditioning of the FRF matrix. Other works have suggested using Bayesian inference regression methods to estimate the forces [12, 13]. These methods can be used to simultaneously perform source selection and regularization to enhance the predictive capability of the forces and reduce the possibility of an overfit.

It is also clear that uncertainty quantification (UQ) methods should be used to provide error bounds on the response predictions so an appropriate specification can be derived from the virtual field data. This is an open area of research with significant previous work to use or build on. Some methods evaluate the uncertainty due to the FRF matrix inversion and measurement noise [14, 15]. Other methods can be used to evaluate the uncertainty when using FE models to estimate the forces or generate the FRFs. The Monte Carlo method, where repeated versions of models with randomly changing variables are used, is a straightforward approach to this problem. Perturbations of the mode frequency and damping could be a simple way to use Monte Carlo. Random matrix theory has also been proposed as a method to develop perturbed versions the system matrices [16, 17]. Additional UQ methods would need to be factored in to quantify the error in the response prediction if classical TPA is being used.

CONCLUSIONS

TPA is being proposed as a method to generate virtual field data for deriving multi-axis vibration test specifications. Early work has shown promising results for both classical and component-based TPA. Component-based TPA is an obvious solution to this problem since the response predictions on new systems theoretically match the actual field environment. The drawback of component-based TPA is that it requires a model of the source system (either FRFs, mode shapes, or an FE model), which are not always available. Classical TPA may provide a useful alternative in these cases because it can be used to map a source environment to the structural dynamics and response DOFs on the DUT. This approach may be beneficial relative to the alternative, which is typically direct application of the original system data to the new system.

Regardless of the promise that TPA shows, future work is required to build trust in the method. The main areas (in the author's opinion) are developing better methods for choosing appropriate FRFs for the inverse force estimation and building UQ into the response predictions. There are several prior works that address these areas, giving cause for optimism on the future use of TPA to develop multi-axis vibration test specifications.

REFERENCES

- [1] R. P. Mayes and D. P. Rohe, "Physical Vibration Simulation of an Acoustic Environment with Six Shakers on an Industrial Structure," in *Shock & Vibration, Aircraft/Aerospace, Energy Harvesting, Acoustics & Optics, Volume 9. Conference Proceeding of the Society for Experimental Mechanics Series*, Springer, Cham, 2016, pp. 29-41.
- [2] D. P. Rohe and R. Schultz, "Rattlesnake: An open-source multi-axis and combined environments vibration controller," in *Proceedings of IMAC-XL, the 40th International Modal Analysis Conference*, Orlando, 2022.
- [3] *MIL-STD 810H, Military Standard, Environmental Test Methods and Engineering Guidelines*, United States Department of Defense, 2019.
- [4] R. Schultz and G. D. Nelson, "Techniques for Modifying MIMO Random Vibration Specifications," in *Proceedings of IMAC-XL, the 40th International Modal Analysis Conference*, Orlando, 2022.
- [5] P. M. Daborn, Smarter Dynamic Testing of Critical Structures, University of Bristol, 2014.
- [6] M. V. van der Seijs, D. de Klerk and D. J. Rixen, "General Framework for Transfer Path Analysis: History, Theory, and Classification of Techniques," *Mechanical Systems and Signal Processing*, Vols. 68-69, pp. 217-244, 2016.
- [7] D. Roettgen, G. Lopp, A. Jaramillo and B. Moldenhauer, "Experimental Substructuring of the Dynamic Substructures Round Robin Testbed," in *Proceedings of IMAC-XL, the 40th International Modal Analysis Conference*, Orlando, 2022.
- [8] A. Linderholt and D. Roettgen, "Substructuring on Combinations of Steel and Aluminum Components of the Benchmark Structure of the Technical Division on Dynamic Substructures," in *Proceedings of IMAC-XL, the 40th International Modal Analysis Conference*, Orlando, 2022.
- [9] S. P. Carter and B. C. Owens, "Errors Using Six Degree of Freedom Force Estimates to Translate Environments System-to-System," in *ISMA 2022*, Leuven, 2022.
- [10] C. Beale, R. Schultz, C. Smith and T. Walsh, "Degree of Freedom Selection Approaches for MIMO Vibration Test Design," in *Proceedings of IMAC-XL, the 40th International Modal Analysis Conference*, Orlando, 2022.
- [11] M. W. F. Wernsen, v. d. S. V. Maarten and D. de Klerk, "An Indicator Sensor Criterion for In-situ Characterisation of Source Vibrations," in *Proceeding of IMAC-XXXV*, 2017.

- [12] M. Aucejo and O. De Smet, "Bayesian Source Identification Using Local Priors," *Mechanical Systems and Signal Processing*, Vols. 66-67, pp. 120-136, 2016.
- [13] M. Aucejo and O. De Smet, "On a Full Bayesian Inference for Force Reconstruction Problems," *Mechanical Systems and Signal Processing*, vol. 104, pp. 36-59, 2018.
- [14] S. Voormeeren, D. de Klerk and D. J. Rixen, "Uncertainty Quantification in Experimental Frequency Based Substructuring," *Mechanical Systems and Signal Processing*, vol. 24, no. 1, pp. 106-118, 2010.
- [15] J. W. Meggit, A. T. Moorhouse and A. S. Elliott, "A Covariance Based Framework for the Propagation of Uncertainty through Inverse Problems with an Application to Force Identification," *Mechanical Systems and Signal Processing*, vol. 124, pp. 275-297, 2019.
- [16] A. Acri, E. Nijman, A. Acri and G. Offner, "Influences of System Uncertainties on the Numerical Transfer Path Analysis of Engine Systems," *Mechanical Systems and Signal Processing*, vol. 95, pp. 106-121, 2017.
- [17] D. C. Kammer, P. Blelloch and J. Sills, "Variational Coupled Loads Analysis Using the Hybrid Parametric Variation Method," in *Model Validation and Uncertainty Quantification, Volume 3. Conference Proceeding of the Society for Experimental Mechanics*, Springer, Cham, 2020.